PHYSICAL REVIEW C **94**, 034304 (2016)

Direct experimental evidence for a multiparticle-hole ground state configuration of deformed ^{33}Mg

Ushasi Datta,[1,2,*] A. Rahaman,[1] T. Aumann,[2,3] S. Beceiro-Novo,[4] K. Boretzky,[2] C. Caesar,[2] B. V. Carlson,[5] W. N. Catford,[6] S. Chakraborty,[1] M. Chartier,[7] D. Cortina-Gil,[4] G. de Angelis,[8] P. Diaz Fernandez,[4] H. Emling,[2] O. Ershova,[2] L. M. Fraile,[9] H. Geissel,[2,10] D. Gonzalez-Diaz,[2] B. Jonson,[11] H. Johansson,[11] N. Kalantar-Nayestanaki,[12] T. Kröll,[3] R. Krücken,[13] J. Kurcewicz,[2] C. Langer,[2] T. Le Bleis,[12] Y. Leifels,[2] J. Marganiec,[2,14] G. Münzenberg,[2] M. A. Najafi,[12] T. Nilsson,[11] C. Nociforo,[2] V. Panin,[2] S. Paschalis,[3] R. Plag,[2] R. Reifarth,[2] V. Ricciardi,[2] D. Rossi,[2] H. Scheit,[3] C. Scheidenberger,[2,10] H. Simon,[2] J. T. Taylor,[7] Y. Togano,[2] S. Typel,[2] V. Volkov,[3] A. Wagner,[15] F. Wamers,[2] H. Weick,[2] M. Weigand,[2] J. S. Winfield,[2] D. Yakorev,[15] and M. Zoric[2]

[1]*Saha Institute of Nuclear Physics, Kolkata 700064, India*
[2]*GSI Helmholtzzentrum für Schwerionenforschung GmbH, D-64291 Darmstadt, Germany*
[3]*Technische Universität Darmstadt, 64289 Darmstadt, Germany*
[4]*Universidade de Santiago de Compostela, 15706 Santiago de Compostela, Spain*
[5]*Instituto Tecnologico de Aeronautica, Sao Jose dos Campos, Brazil*
[6]*University of Surrey, Guildford GU2 5XH, United Kingdom*
[7]*University of Liverpool, Liverpool L69 7ZE, United Kingdom*
[8]*INFN, LNL, Legnaro, Italy*
[9]*Universidad Complutense de Madrid, Avenida Complutense, E-28040 Madrid, Spain*
[10]*Physikalisches Institut, Giessen, Germany*
[11]*Fundamental Fysik, Chalmers Tekniska Hogskola, S-412 96 Goteborg, Sweden*
[12]*KVI-CART, University of Groningen, The Netherlands*
[13]*Physik Department E12, Technische Universität München, 85748 Garching, Germany*
[14]*EMMI, GSI Helmholtzzentrum für Schwerionenforschung GmbH, D-64291 Darmstadt, Germany*
[15]*Helmholtz-Zentrum Dresden-Rossendorf, D-01328 Dresden, Germany*

(Received 12 June 2014; revised manuscript received 2 June 2016; published 6 September 2016)

The first direct experimental evidence of a multiparticle-hole ground state configuration of the neutron-rich ^{33}Mg isotope has been obtained via intermediate energy (400 A MeV) Coulomb dissociation measurement. The major part $\sim(70 \pm 13)\%$ of the cross section is observed to populate the excited states of ^{32}Mg after the Coulomb breakup of ^{33}Mg. The shapes of the differential Coulomb dissociation cross sections in coincidence with different core excited states favor that the valence neutron occupies both the $s_{1/2}$ and $p_{3/2}$ orbitals. These experimental findings suggest a significant reduction and merging of sd-pf shell gaps at $N \sim 20$ and 28. The ground state configuration of ^{33}Mg is predominantly a combination of ^{32}Mg(3.0,3.5 MeV; 2^-,1^-) $\bigotimes \nu_{s_{1/2}}$, ^{32}Mg(2.5 MeV; 2^+) $\bigotimes \nu_{p_{3/2}}$, and ^{32}Mg($0; 0^+$) $\bigotimes \nu_{p_{3/2}}$. The experimentally obtained quantitative spectroscopic information for the valence neutron occupation of the s and p orbitals, coupled with different core states, is in agreement with Monte Carlo shell model (MCSM) calculation using 3 MeV as the shell gap at $N = 20$.

DOI: 10.1103/PhysRevC.94.034304

I. INTRODUCTION

The observation of the breakdown of traditional magic numbers [1] in exotic nuclei far from the β-stability line has been an important issue in nuclear structure physics and significant effort has been put into both experimental investigations [2–12] and theoretical studies [13–16]. The first observation of the disappearance of the so-called magic number was reported by Thibault *et al.* [2], based on mass measurements of the neutron-rich ^{31,32}Na isotopes [2]. Later a similar observation was also reported for ^{33}Mg [3]. The onsets of deformations in the nuclei ^{32}Mg [4], ^{31}Na [5], and ^{30}Ne [7] at $N = 20$ shell closure were also observed. These phenomena were proposed to originate due to substantial contributions from so-called intruder pf configurations over the normal sd shell in the ground state wave functions. It is possible that the sd-pf shell gap ($N = 20$) is reduced. The $N = 20$ isotones for $Z \sim$ 10–12 are considered to belong to the so-called island of inversion [13]. The breakdown of the $N = 20$ shell gap can be explained by the nucleon-nucleon interaction (strongly attractive monopole interaction of the tensor force) [14,15]. Fortune [16] has shown that the measured data on the reduced matrix element of the first excited 2^+ state of the ^{32}Mg [4] can be explained by a dominant sd-shell configuration in the ground state of this isotope.

Hence, it is important to study detailed shell configurations of the ground state of the neutron-rich $N = 21$ isotones. Many different experiments [3,6,8–12] have been performed to unravel the structure of ^{33}Mg ($N = 21$) but until now neither the ground state parity nor the shell configuration has been confirmed. From the measured negative sign of the magnetic moment, a pure $3p$-$2h$ ground state configuration and $3/2^-$ ground state spin and parity were suggested [10]. In contrast, $3/2^+$ ground state spin and parity with a $4p$-$3h$ or $2p$-$1h$ configuration was assigned through β-decay measurements,

*ushasi.dattapramanik@saha.ac.in

i.e., ^{33}Mg to ^{33}Al [9] and ^{33}Na to ^{33}Mg [6]. A narrow longitudinal momentum distribution (150 ± 3 MeV/c) of ^{32}Mg was observed in the knockout reaction of this ($S_n = 2.22$ MeV) nucleus [11]. The measured longitudinal momentum distribution was in good agreement with both ground state spin of either $3/2^+$ or $3/2^-$, considering mixed configurations of ^{32}Mg in excited states coupled with a neutron in the sd-pf shell [11,12]. In this article, we report the first direct experimental evidence for a multiparticle-hole ground state configuration of the neutron-rich ^{33}Mg isotope, and significant reduction as well as merging of the sd-pf shell gaps at $N = 20$ and 28, obtained via intermediate energy (400 A MeV) Coulomb dissociation measurements. This article reports detailed major components of the ground state configuration of this neutron-rich nucleus with an original view of its exotic structure.

II. EXPERIMENT AND ANALYSIS

The experiment (GSI: S306) was performed using the FRS-ALADIN-LAND setup at GSI Helmholtz Centre for Heavy Ion Research in Germany, Darmstadt. The radioactive beam, ^{33}Mg, was produced by fragmentation of an ^{40}Ar beam of energy 540 A MeV. After the separation by the fragment separator (FRS) [17], the beam (∼2% of the total cocktail beam at the reaction target) was transported to the experimental site, where complete kinematic measurements were performed using secondary ^{208}Pb and ^{12}C targets and an empty target. The target was surrounded by 160 NaI detectors used for detecting the γ rays from the excited nuclei. The γ rays were reconstructed through the add-back procedure among neighboring crystals of highest energy deposition followed by Doppler correction. The γ-sum energy spectra was obtained by adding the coincident γ rays. A detailed response corresponding to detection of the γ-rays has been generated using the Monte Carlo code (GEANT). The detection efficiencies of the γ rays under the experimental condition have been estimated by the GEANT simulation. Validation of the simulated results has been performed by comparing the experimental data of standard calibrated γ-ray sources with the simulated one. The efficiency of the sum-energy spectra of simulated and experimental data are in agreement within 10%. After the reaction at the secondary target, the reaction fragments as well as the unreacted beam were bent by a large dipole magnet and ultimately detected at the time-of-flight wall detector. By the use of energy-loss and time-of-flight measurements, as well as position measurements in front and behind the dipole magnet, the nuclear charge, velocity, scattering angle, and mass of the fragments were determined. The emitted neutrons from the excited projectile were forward focused and tracked with the Large Area Neutron Detector [18]. For details of the setup, see Refs. [19–21].

The excitation energy E^* of the projectile, ^{33}Mg, prior to decay is obtained by reconstructing the invariant mass by measuring the four momenta of all the decay products of the projectile after breakup [22–25]. The Coulomb dissociation (CD) cross section for the ^{208}Pb target (2.0 g/cm^2) has been determined after subtracting the nuclear contribution, which was estimated from the data for a ^{12}C target (0.9 g/cm^2) with proper scaling factor (1.8) [26].

The experimental data on the electromagnetic excitation to the nonresonant continuum has been analyzed using the direct breakup model to explore the ground state configuration [22–25,27].

III. COULOMB BREAKUP

When a projectile passes by a high-Z target, it may be excited by absorbing virtual photons from the time-varying Coulomb field and subsequently breakup into a neutron and core. This one-neutron-removal differential Coulomb dissociation (CD) cross section can be expressed as an incoherent sum of the components of $d\sigma_c^\pi/dE^*$ corresponding to the different the spin and parity core states populated after breakup. This can be expressed through the following equation [22]:

$$\frac{d\sigma_c^\pi}{dE^*} = \frac{16\pi^3}{9\hbar c} N_{E1}(E^*) \sum_j C^2S\left(I_c^\pi, nlj\right) \times \sum_m \left|\langle q|(Ze/A) r Y_m^l|\psi_{nlj}(r)\rangle\right|^2, \quad (1)$$

where $N_{E1}(E^*)$ is the number of virtual photons as a function of the excitation energy E^* [28]. $\psi_{nlj}(r)$ and $\langle q|$ represent the single-particle wave function of the valence neutron in the projectile ground state and the final state wave function of the valence neutron in the continuum, respectively. The single-particle wave functions are calculated in a Wood-Saxon potential with radius $r_0 = 1.25$ fm and diffuseness $a = 0.7$ fm. The outgoing neutron wave function in the continuum is considered to be a plane wave. $C^2S(I_c^\pi, nlj)$ represents the spectroscopic factor with respect to a particular core state I_c^π of the valence neutron in the projectile ground state.

By comparing the experimental CD cross section with the calculated one, information on the ground state properties, such as the orbital angular momentum of the valence nucleon and the corresponding spectroscopic factor, may be obtained. The core state, which is coupled with the neutron, can be identified by the characteristic γ rays from the decaying core after the breakup. In order to compare with the experimental results, all the calculated results shown in this article are convoluted with the response function [24,29].

IV. RESULTS AND DISCUSSION

The total inclusive Coulomb dissociation cross section for $^{33}\text{Mg} \rightarrow {}^{32}\text{Mg} +$ neutron, integrated up to 9 MeV excitation energy, amounts to 106 ± 14 mb. Figure 1 shows the total CD cross section for $^{33}\text{Mg} \rightarrow {}^{32}\text{Mg} + n$. No resonance-like structure is observed in the excitation spectra of ^{33}Mg (Fig. 1). The total inclusive experimental differential CD cross section has been fitted using the calculated one. The insets of Fig. 1 (left) and Fig. 1 (right) show the χ^2/N for fitting with variation of the valence neutron spectroscopic factor in the s and p orbitals, respectively. The best fit suggests that the valence neutron coupled with ^{32}Mg (0^+) in the ground state cannot explain the data.

Figure 2 (top) shows the sum-energy spectrum of the γ rays decaying from the excited states of ^{32}Mg after Coulomb breakup of ^{33}Mg. This spectrum is obtained in coincidence

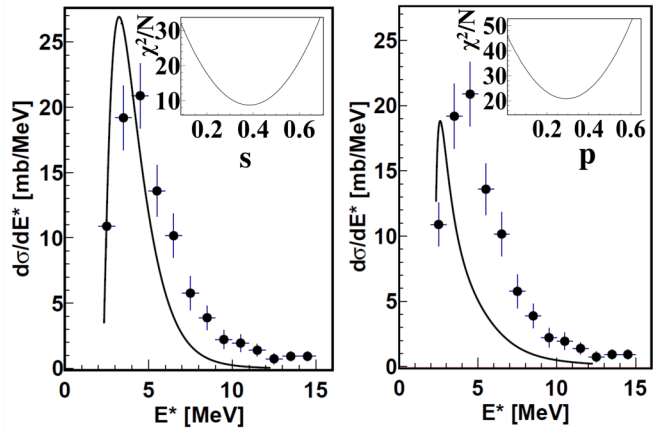

FIG. 1. Total inclusive differential CD cross section with respect to the excitation energy (E^*) of ^{33}Mg. The smooth curve is the cross section on the basis of a direct breakup model using a plane wave approximation for the s (left panel) and the p orbital (right panel) neutrons, respectively. The inset of the each panel of the figure shows the χ^2/N for the fit of the direct breakup model calculation to the experimental differential CD.

with the incoming beam ^{33}Mg, the outgoing fragment ^{32}Mg, and one neutron. This spectrum reflects the ground state configuration of ^{33}Mg as the reaction mechanism demands [22]. The γ-ray spectra from reactions with high-energy projectiles on high-Z targets are strongly affected (up to energies of a few MeV) by the low-energy background. This background originates from atomic interactions of the beam with the lead target [30]. The shape of the low-energy background was obtained from the γ-ray spectrum in coincidence with the noninteracting Mg beam [spectrum I in Fig. 2 (bottom)]. To understand the sum-energy spectra of the γ ray, a detailed response corresponding to detection of the sum-energy spectrum of the γ rays decaying from a particular excited state in the experimental situation has been generated using the GEANT code. Spectra II, III, and IV in Fig. 2 (bottom) are the simulated sum-energy spectra of γ rays decaying from the 2.5-MeV excited state, a combination of the 3.0- and 3.5-MeV states, and a combination of the 4.78- and 4.82-MeV states, respectively. In the simulation, the decay scheme of various excited states of ^{32}Mg were considered as reported in the literature [31] and the partial level schemes of ^{32}Mg are shown in the inset of Fig. 2 (top). The solid (black online) line in Fig. 2 (bottom) represents the sum of spectra I, II, III, and IV. The partial Coulomb breakup cross sections of ^{33}Mg for populating various excited states of ^{32}Mg have been extracted from the invariant mass spectra in coincidence with the sum energy of γ rays in the three different above mentioned regions. The detection efficiency and feeding corrections from higher states of γ rays have been obtained from detailed simulations. The detection efficiencies of the sum energy of γ rays from 2.3 to 2.8, 2.9 to 4.0, and 4.0 to 5.7 MeV are $41 \pm 4\%$, $41 \pm 4\%$, and $47 \pm 5\%$, respectively. Thus partial CD cross sections for populating the above three sets of excited states of ^{32}Mg are 23 ± 5, 34 ± 6, and 17 ± 6 mb. These cross sections are obtained from the Pb-target data after subtracting its nuclear part. The cross

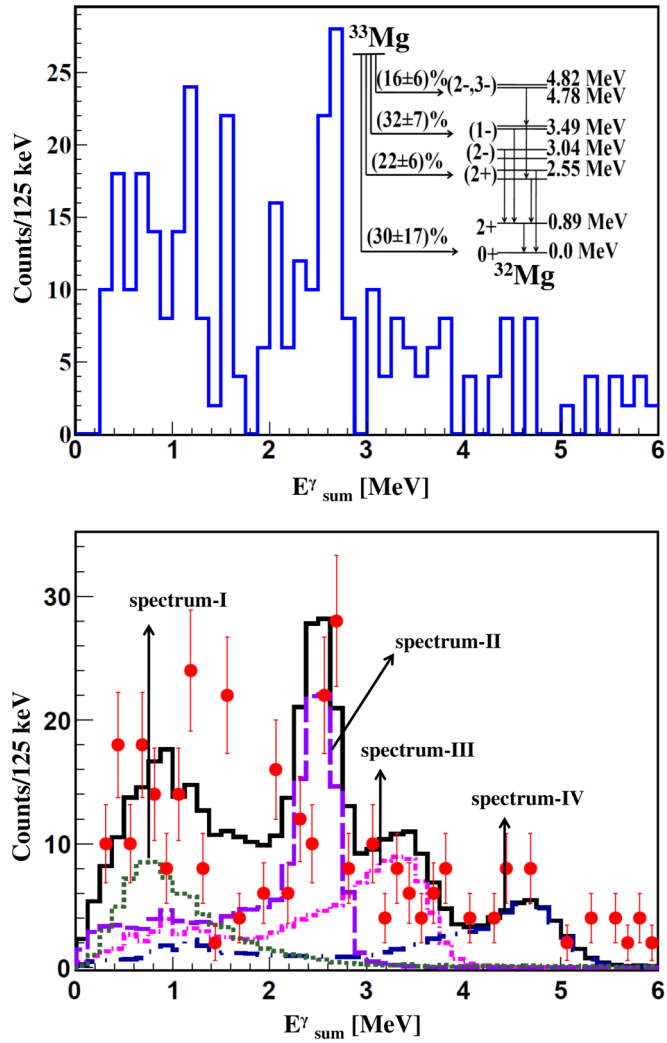

FIG. 2. (Top) The observed sum-energy spectrum of γ-ray transitions from the excited states of ^{32}Mg after Coulomb breakup of ^{33}Mg. The inset shows a partial scheme of levels in ^{32}Mg and the population of those states after Coulomb breakup. (Bottom) The solid black line represents the sum of simulated sum-energy spectra of γ rays decaying from various core excited states and experimental atomic background. The experimental atomic background is represented by spectrum I. Spectrum II, spectrum III, and spectrum IV represent the simulated sum-energy spectra of γ rays decaying from the 2.5-MeV excited state and combinations of the 3.5- and 3.0-MeV states and the 4.78- and 4.82-MeV states, respectively.

section for the ground state is 32 ± 17 mb, which is obtained from the difference between the total CD cross section and the cross sections of the excited states. The inset of Fig. 2 (top) shows the relative population of different core excited states after Coulomb breakup. Thus the data analysis shows that the overwhelming part $\sim(70 \pm 13)\%$ of the cross section leaves the core, ^{32}Mg, in its excited states.

It is interesting to note that after the Coulomb breakup of ^{17}C, a major part ($\sim$91%) of the core, ^{16}C, also populates excited states [22] and that the ground-state spin, parity, and single-particle configuration of ^{17}C, obtained from the Coulomb breakup analysis [22], are in agreement with the

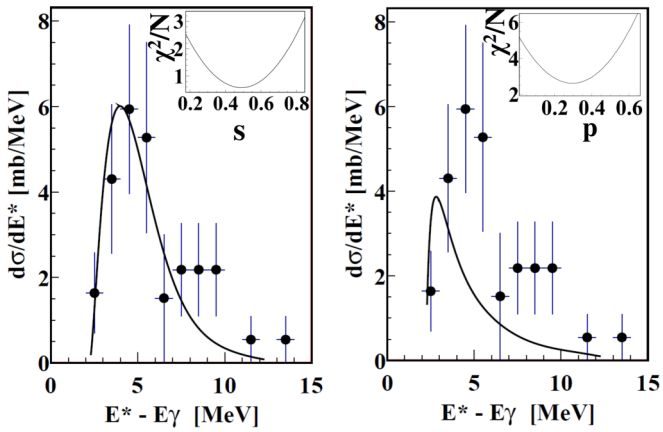

FIG. 3. Partial differential CD cross section of ^{33}Mg with respect to (E^*-E_γ) in coincidence with ^{32}Mg in the excited states ∼3.0, 3.5 MeV ($I^\pi = 1^-,2^-$). The smooth curve is the cross section on the basis of the direct breakup model using a plane wave approximation for the s-wave (left) and the p-wave (right) neutron, respectively. The inset of each panel of the figure shows the χ^2/N for the fit.

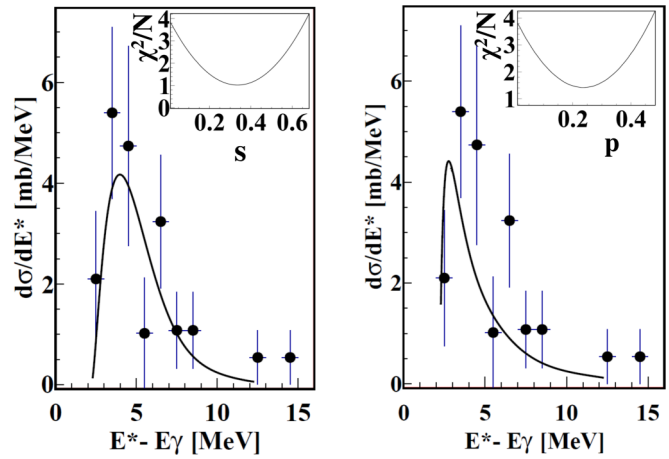

FIG. 4. Partial differential CD cross section of ^{33}Mg with respect to (E^*-E_γ), in coincidence with ^{32}Mg in the excited state ∼2.5 MeV ($I^\pi = 2^+$). The smooth curve is the cross section on the basis of the direct breakup model using a plane wave approximation for the s orbital (left panel) and p orbital (right panel). The inset of each panel of figure shows the χ^2/N for the fit.

knockout reaction [32]. The present analysis of Coulomb breakup of ^{33}Mg has been performed in a similar manner to that of ^{17}C [22].

The ground-state spin of ^{33}Mg is 3/2 as suggested by two recent independent experiments [9,10]. But the parity and the single-particle configuration are under debate. To explore further this issue, further data analysis has been performed. Figure 3 shows the differential CD cross section in coincidence with the sum-energy γ-rays of ∼3.5 and 3.0 MeV. The data have been fitted with the direct breakup model calculation. The left and right insets of Fig. 3 show the variation of χ^2/N as a function of the spectroscopic factor of the valence neutron, occupying the s and p orbitals, respectively. The χ^2/N for the fit clearly suggests that the valence neutron occupies the s orbital with the spectroscopic factor 0.47 ± 0.08. Even for 4σ error (i.e, within a 99.99% confidence limit), the spectroscopic factor would be between 0.15 to 0.8. In contrast, a similar analysis in coincidence with the sum-energy γ rays of 2.5 MeV can explain the data with the neutron occupying either the s or p orbitals. Figure 4 shows the differential CD cross section in coincidence with the γ decay of energy ∼2.5 MeV. This can be understood by noting that the 2.5-MeV γ ray can be obtained from de-excitation of the 3.5 MeV (1^-) state as well as the 2.5-MeV (2^+) state, which are of opposite parity states. Similar to that above, the spectroscopic factor of 0.26 ± 0.07 can be obtained for the valence neutron occupying a p orbital coupled with ^{32}Mg(2.5 MeV; 2^+). Unlike the other two situations, for the cross section with large statistical error, i.e., $^{32}\mathrm{Mg}(0.0^+) \bigotimes \nu_{p_{3/2}}$, the spectroscopic factor is obtained from the ratio of the experimental cross section to the calculated one. Thus, different components of the ground-state configuration of this nucleus are $^{32}\mathrm{Mg}(3.0\,\mathrm{MeV},3.5\,\mathrm{MeV}; 1^-,2^-) \bigotimes \nu_{s_{1/2}}$, $^{32}\mathrm{Mg}(2.5\ \mathrm{MeV}; 2^+) \bigotimes \nu_{p_{3/2}}$, and $^{32}\mathrm{Mg}(0; 0^+) \bigotimes \nu_{p_{3/2}}$. This suggests that the ground-state parity is negative and the spin could be 3/2, which was proposed earlier [9,10]. Considering this spin and parity, a tentative fourth component of the ground-state configuration can be considered as ^{32}Mg(4.78 MeV, 4.82 MeV; 2^-) $\bigotimes \nu_{s_{1/2}}$. Since the exclusive CD cross section associated with this core state is small with large error, the spectroscopic factor (0.37 ± 0.13) for the valence neutron in the $s_{1/2}$ orbital can be obtained from ratio of the cross sections. It is interesting to note that measurements of both the magnetic moment [33] and the Coulomb breakup [21] of the neutron-rich isotope ^{34}Al ($N = 21$) support a multiparticle-hole ground state configuration.

In Fig. 5, the summation of the four exclusive calculated CD cross sections for the four above-mentioned components

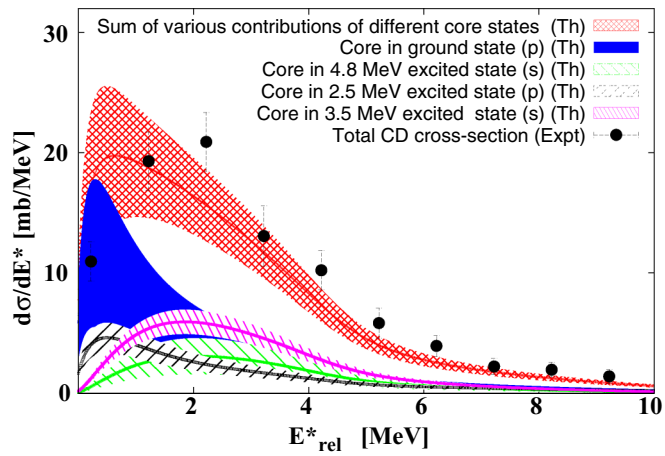

FIG. 5. The total experimental inclusive (black filled-circle data) differential CD cross section of ^{33}Mg is overlaid with the sum of calculated exclusive CD cross sections (red solid line) for four components of the ground state. The (red online) mesh shaded region is the associated errors obtained from the various contributions. Other shaded regions as mentioned in the figure represent different calculated exclusive CD cross sections with errors. The error of each component is obtained from the respective error of the spectroscopic factor of valence neutron(s), occupying a particular orbital coupled with the core excited state as shown in the figure.

TABLE I. Partial Coulomb dissociation cross sections of ^{33}Mg for different core states up to excitation energy ($E_c + 9.0$) MeV. The corresponding spectroscopic factors from calculations [11] and the ones derived from the experiment are quoted.

Core state I^π (E_c MeV)		Neutron orbital	Cross section (mb)	Spectroscopic factor	
				Shell	Experiment
Experiment [31]	Calculated [11]			model [11]	
0^+ (0.0)	0^+ (0.0)	$1p_{3/2}$	32 ± 17	0.12	0.19 ± 0.1
2^+(2.5)		$1p_{3/2}$	23 ± 5		0.26 ± 0.07
	2^+(3.01)			0.2	
2^-(3.0)		$1s_{1/2}$			
1^-(3.49)		$1s_{1/2}$	34 ± 6		0.47 ± 0.08
	1^-(3.81)	$1s_{1/2}$		0.21	
	2^- (3.94)	$1s_{1/2}$		0.27	

of the ground state configuration is overlaid with the inclusive total experimental differential Coulomb breakup cross section (black filled circles) of ^{33}Mg. The mesh (red online) shaded region represents the associated error obtained from the various contributions. A good agreement between data and calculation provides validation of the ground state configuration, obtained from different components of exclusive CD data. The shaded regions with closely spaced left-tilted lines (pink online), right-tilted lines (black online), widely spaced left-tilted lines (green online), and solid-filled shaded region represent the calculated differential CD cross sections for the configurations of ^{32}Mg(3.0 MeV, 3.5 MeV; $1^-, 2^-$) $\bigotimes \nu_{s_{1/2}}$, ^{32}Mg(2.5 MeV; 2^+) $\bigotimes \nu_{p_{3/2}}$, ^{32}Mg(4.8 MeV; 2^-) $\bigotimes \nu_{s_{1/2}}$, and ^{32}Mg($0; 0^+$) $\bigotimes \nu_{p_{3/2}}$, respectively. These differential CD cross sections are multiplied by the experimental spectroscopic factors and associated errors.

Table I shows the partial experimental Coulomb dissociation cross sections of ^{33}Mg for different core states with the spectroscopic factor for valence neutron occupation. The corresponding spectroscopic factors from Monte Carlo shell model (MCSM) calculations with SDPF-M interaction [11,34] are shown in the fifth column of the table. The SDPF-M interaction is combination of USD interaction for sd shell, the Kuo-Brown interaction for pf shell and a modified Millener-Kurath interaction for the cross shell. The experimental results are in good agreement with the calculation. It is evident from the table that a large spectroscopic factor is obtained for the valence neutron ($N = 21$) in the $s_{1/2}$ orbital. It was shown through shell model calculations that multiparticle-hole (np-nh) excitations across the shell gap may lead to deformation in this region [13]. The reaction data [8] support prolate deformation of this isotope. The occupation of the valence neutron ($N = 21$) in the $s_{1/2}$ orbital is possible with a large deformation ($\beta_2 \sim 0.45$–0.5) where the extruder $1/2[200]$ deformed Nilsson state with a 60–70% component of the $j = 1/2$ orbital is available near the Fermi level [35].

It was shown by Ripka and Larry [36] that the measured magnetic moments in odd-A nuclei of this mass region deviate from the Schmidt values. But those experimental values could be explained by a calculation using an odd nucleon coupled with a deformed Hartree-Fock core [36]. Similarly, a valence neutron occupying a $1/2[200]$ deformed Nilsson orbital can explain the recently measured magnetic moments of ^{33}Mg [10]. It has been shown that magnetic moment calculated by a particle plus rotor with deformation 0.45 for the $1/2[200]$ state is $-0.86\ \mu_N$ [37] and this value is in agreement with the measured value of $-0.7456(5)\ \mu_N$ [10]. With this deformation, both $1/2[330]$ and $3/2[321]$ deformed intruder Nilsson states with components of the $p_{3/2}$ orbital are available near the Fermi level. And indeed, an experimental signature for the occupation of the p orbital by the valence neutron has been observed in the present experiment.

One can conclude from the analysis of Coulomb breakup data that the ground state configuration of ^{33}Mg is mainly a deformed multiparticle-hole core, ^{32}Mg, coupled with a valence neutron(s) in the deformed Nilsson $1/2[200]$ and $3/2[321]$ states. A number of theoretical investigations have been performed to explore the effect of deformation on the structure of the exotic nuclei [35,38,39]. In the present scenario, the Nilsson states consist mainly of low-l orbital components at high deformation in the loosely bound nucleus [38]. Due to occupation of the state $1/2[200]$ by the valence neutron, one may expect a decoupled band structure of ^{33}Mg, where the particle is decoupled from the core, ^{32}Mg. The deformation in this nucleus can be defined by the intrinsic structure of the weakly bound neutron orbital, by the shape of the core, or by the interplay of both. Thus a rich variety of shape co-existence phenomena or structures are expected to be observed. The shape of the spatial distribution of ^{33}Mg may be different than that of the core, ^{32}Mg. A detailed experimental and theoretical investigation of this nucleus may provide important information about the exotic structure of deformed, multi-quasi-particle neutron-rich nucleus.

V. CONCLUSIONS

In conclusion, the present experimental data of the Coulomb dissociation of ^{33}Mg ($N = 21$) provides the first evidence of a multiparticle-hole ground state configuration and the valence neutron(s) is occupying the s and p orbitals. These observations confirm significant reduction and merging of shell gaps, at $N = 20$ and 28 for this neutron-rich nucleus. The valence neutron of this isotope occupies partially the $s_{1/2}$ orbital, which is an indirect evidence of large deformation ($\beta_2 \sim 0.45$) because the extruder $1/2[200]$ is only available near the Fermi level for $N = 21$. Thus, through the electric dipole response from the ground state to the continuum, a large deformation as well as multiparticle-hole ground state configurations can be obtained for ^{33}Mg. It will be interesting to study the exotic shape evolution of the neutron-rich nuclei near traditional magic numbers using future facilities like FAIR, FRIB, HIE-ISOLDE, and RIBF.

ACKNOWLEDGMENTS

The authors wish to thank the accelerator staff of GSI for their active support during the experiment. Ushasi Datta acknowledges the Alexander von Humboldt Foundation and SEND project (PIN:11-R&D-SIN-5.11-0400), Govt. of India,

for their support of the experimental investigation and is also grateful to Prof. B. M. Sherrill, NSCL, and Prof. Larry Zamick, Rutgers University, for many valuable suggestions and discussion.

[1] M. Geoppert Mayer, Phys. Rev. **75**, 1969 (1949); O. Haxel, *ibid.* **75**, 1766 (1949).
[2] C. Thibault *et al.*, Phys. Rev. C **12**, 644 (1975).
[3] N. A. Orr *et al.*, Phys. Lett. B **258**, 84 (1991); X. G. Zhou *et al.*, Phys. Lett. **260B**, 285 (1991).
[4] T. Motobayashi *et al.*, Phys. Lett. B **346**, 9 (1995).
[5] B. V. Pritychenko *et al.*, Phys. Rev. C **63**, 011305(R) (2000).
[6] S. Nummela *et al.*, Phys. Rev. C **64**, 054313 (2001).
[7] Y. Yanagisawa *et al.*, Phys. Lett. B **566**, 84 (2003).
[8] Z. Elekes *et al.*, Phys. Rev. C **73**, 044314 (2006).
[9] V. Tripathi *et al.*, Phys. Rev. Lett. **101**, 142504 (2008).
[10] D. T. Yordanov *et al.*, Phys. Rev. Lett. **99**, 212501 (2007).
[11] R. Kanungo *et al.*, Phys. Lett. B **685**, 253 (2010).
[12] G. Neyens, Phys. Rev. C **84**, 064310 (2011).
[13] E. K. Warburton, J. A. Becker, and B. A. Brown, Phys. Rev. C **41**, 1147 (1990).
[14] A. De. Shalit *et al.*, Phys. Rev. **92**, 1211 (1953).
[15] T. Otsuka, T. Suzuki, M. Honma, Y. Utsuno, N. Tsunoda, K. Tsukiyama, and M. Hjorth-Jensen, Phys. Rev. Lett. **104**, 012501 (2010).
[16] H. T. Fortune, Phys. Rev. C **85**, 014315 (2012).
[17] H. Geissel *et al.*, Nucl. Instrum. Methods Phys. Res., Sect. B **70**, 286 (1992).
[18] T. Blaich *et al.*, Nucl. Instrum. Methods Phys. Res., Sect. A **314**, 136 (1992).
[19] C. Caeser *et al.*, Phys. Rev. C **88**, 034313 (2013).
[20] A. Rahaman *et al.*, EPJ Web Conf. **66**, 02087 (2014).
[21] S. Chakraborty *et al.*, EPJ Web Conf. **66**, 02019 (2014).
[22] U. Datta Pramanik *et al.*, Phys. Lett. B **551**, 63 (2003).
[23] R. Palit *et al.*, Phys. Rev. C **68**, 034318 (2003).
[24] C. Nociforo *et al.*, Phys. Lett. B **605**, 79 (2005).
[25] U. Datta Pramanik, Prog. Part. Nucl. Phys. **59**, 183 (2007).
[26] C. J. Benesh, B. C. Cook, and J. P. Vary, Phys. Rev. C **40**, 1198 (1989).
[27] T. Aumann and T. Nakamura, Phys. Scr., T **152**, 014012 (2013).
[28] C. A. Bertulani and G. Baur, Phys. Rep. **163**, 299 (1988).
[29] K. Boretzky *et al.*, Phys. Rev. C **68**, 024317 (2003).
[30] R. Anholt *et al.*, Phys. Rev. A **33**, 2270 (1986).
[31] http://www.nndc.bnl.gov
[32] V. Maddalena *et al.*, Phys. Rev. C **63**, 024613 (2001).
[33] P. Himpe *et al.*, Phys. Lett. B **658**, 203 (2008).
[34] Y. Utsuno, T. Otsuka, T. Mizusaki, and M. Honma, Phys. Rev. C **64**, 011301(R) (2001).
[35] I. Hamamoto, Phys. Rev. C **69**, 041306(R) (2004).
[36] G. Ripka and L. Zamick, Phys. Lett. **23**, 347 (1966).
[37] D. T. Yordanov, K. Blaum, M. De Rydt, M. Kowalska, R. Neugart, G. Neyens, and I. Hamamoto, Phys. Rev. Lett. **104**, 129201 (2010).
[38] T. Misu, W. Nazarewicz, and A. Aberg, Nucl. Phys. A **614**, 44 (1997).
[39] F. M. Nunes, Nucl. Phys. A **757**, 349 (2005).